

Received: 2014.11.19  
Accepted: 2014.11.25  
Published: 2014.12.10

# Suitability of the Rat Subdermal Model for Tissue Engineering of Heart Valves

Authors' Contribution:  
Study Design A  
Data Collection B  
Statistical Analysis C  
Data Interpretation D  
Manuscript Preparation E  
Literature Search F  
Funds Collection G

ABCDEF **Torsten Christ**  
ADEF **Pascal M. Dohmen**  
AB **Sebastian Holinski**  
BD **Melanie Schönau**  
B **Georg Heinze**  
ADE **Wolfgang Konertz**

Department of Cardiovascular Surgery, Charité-Universitätsmedizin Berlin, Berlin, Germany

**Corresponding Author:** Torsten Christ, e-mail: [torsten.christ@charite.de](mailto:torsten.christ@charite.de)  
**Source of support:** Departmental sources

**Background:** Tissue engineering (TE) is a promising approach to overcome problems associated with biological heart valve prosthesis. Currently several animal models are used to advance this method. The rat subdermal model is uncomplicated and widely used, but its suitability for TE has not yet been shown.

**Material/Methods:** Using the rat subdermal model we implanted two decellularized porcine aortic wall specimens (of which one was endothelialized) and one native porcine aortic wall specimen in 30 Lewis rats, respectively. Endothelial cells (EC) were harvested from the rat jugular veins. After explantation Hematoxylin/Eosin-staining, CD-68-positive cell staining, fibroblast-staining and Von-Willebrand factor staining were performed.

**Results:** All animals survived without complications. Endothelialization was confirmed to be effective by Giemsa staining. Histological evaluation of specimens in Hematoxylin/Eosin staining showed significant decrease ( $p < 0.05$ ) of inflammatory reaction (confirmed by CD-68-positive cell staining) after decellularization. All specimens showed strongest inflammatory reactions at areas of destroyed extracellular matrix. Fibroblasts could be detected in all specimens, with strongest infiltration in decellularized specimens ( $p < 0.05$ ). Surrounding endothelialized specimens had no monolayer of endothelial cells, but a higher density of blood vessels occurred ( $p < 0.05$ ).

**Conclusions:** The subdermal model provides excellent contact of host tissue with implanted specimens leading to rapid cellular infiltration; therefore, we could ascertain reduced inflammatory response to decellularized tissue. Due to the subdermal position, an absence of blood stream and mechanical stress occurs, which influences cellular repopulation; therefore, endothelialization did not lead to an EC monolayer, but rather to increased vascularization. Thus, the model appears ideal for investigating basic biological compatibility, but further questions must be researched using other models.

**MeSH Keywords:** **Heart Valve Prosthesis • Heart Valves • Models, Animal • Tissue Engineering**

**Full-text PDF:** <http://www.basic.medscimonit.com/abstract/index/idArt/893088>

 2375  —  4  18



## Background

Tissue engineering (TE) is a promising approach to overcome problems associated with glutaraldehyde-fixed biological heart valve prosthesis, such as calcification, degeneration, and resulting re-operations [1]. In recent years many studies have investigated tissue engineering of heart valves. One major topic is finding an optimal scaffold that shows no antigenic potential and allows immigration of host cells. Ultimately, the scaffolds should allow *in vivo* repopulation of the tissue in heart valves, which in that way are able to remodel, and regenerate and have growth potential [2–4]. The recellularization of the scaffolds, in which fibroblasts and endothelial cells (EC) play a major role, is of special importance. Various animal models are in use to study tissue engineered heart valves [5]. Study setups with juvenile sheep are widely used because tests can be done in the systemic circulation [6]. However, these experiments are complex, time-consuming, and expensive. Easier and less expensive study setups as a first step in developing tissue-engineered heart valves are needed. The rat subdermal model offers these advantages [5] It has been used widely in studies with tissue of conventional heart valves regarding calcification and cellular infiltration [7]. The feasibility of this method in tissue-engineered heart valves remains to be confirmed.

## Material and Methods

All experiments were performed in accordance with the Principles of Laboratory Animal Care prepared by the National society of Medical Research and the Guide for the Care and Use of Laboratory Animals prepared by the Institute of Laboratory Animal Resource and published by the National Institute of Health (NIH Publ. 85-23, Rev 1985). The study was approved by the Ethics Committee of Charité – Medical University Berlin.

The basic principle of the study is the implantation of tissue specimens in Lewis rats in a subdermal position according to the technique of Mako [7]. Tissue specimens measuring 1 cm<sup>2</sup> were cut from porcine aortic walls. Three different groups of tissue specimens were implanted: Group 1: decellularized and endothelialized specimens; Group 2: decellularized specimens; Group 3: native specimens (serving as control).

### Preparation of the tissue specimens

After trimming, the tissue specimens of group 1 and 2 were decellularized. The tissue specimens of group 3 were stored in antibiotic solution. Decellularization was performed as previously described by Dohmen et al. [8]. After decellularization, the tissue was stored in antibiotic solution. For isolation and cultivation of EC, jugular veins were harvested from 30 Lewis

rats. Jugular veins were filled with collagenase to disassociate EC from vein walls. The resulting dilution was used to cultivate EC, as published by Dohmen et al. [8]. Growth of the EC culture was controlled daily by light microscopy. Decellularized tissue specimens were endothelialized as previously described [8]. Efficiency of endothelialization was controlled by Giemsa staining.

### Explantation of tissue specimens

From 10 rats, specimens were explanted after 2 weeks, from another 10 rats after 4 weeks, and from the last 10 rats after 6 weeks. The subcutaneous pockets at the back of the laboratory animals were re-opened and specimens were removed along with surrounding tissue. Afterwards, gross examination of specimens was performed (signs of inflammation, blood vessel ingrowth, encapsulation, and accumulation of ichor) and rats were sacrificed. Ninety tissue specimens could be explanted for analyses.

### Histology

Tissue specimens were all preserved in formalin and embedded in paraffin. Longitudinal sections were made from the middle of the specimens. Afterwards, histological examination was performed to observe the cellular repopulation using a Leica DM 1000 microscope. Pictures were taken using a Leica DSC 290 camera. Examination was performed at the former intimal and adventitial side of the aortic tissue and at the cutting edge of the tissue specimens. For evaluation, a representative section of the respective part of the tissue specimens was chosen, using a lens-coverage of 1:400. The following methods were used for histological examination of the implanted tissue.

#### Light microscopy

Hematoxylin-eosin staining was performed on all specimens to allow general evaluation of cellular infiltration. For determination of the grade of infiltration, the sections were analyzed using the following scale: 0=no infiltration, 1=low infiltration, 2=medium infiltration, 3=high infiltration.

#### Immunohistochemistry

Staining for fibroblasts (Prolyl-4-hydroxylase, clone 6-9H6), monocytes, and macrophages (CD 68, clone KP1) was performed to evaluate the grade of respective infiltration using the following scale: 0=no infiltration, 1=low infiltration, 2=medium infiltration, 3=high infiltration. Staining for Von Willebrand Factor was performed to identify EC and to evaluate the density of blood vessels surrounding the tissue specimens using the following scale: 0=no vessels, 1=1–4 vessels, 2=4–8 vessels, 3=more than 8 vessels.

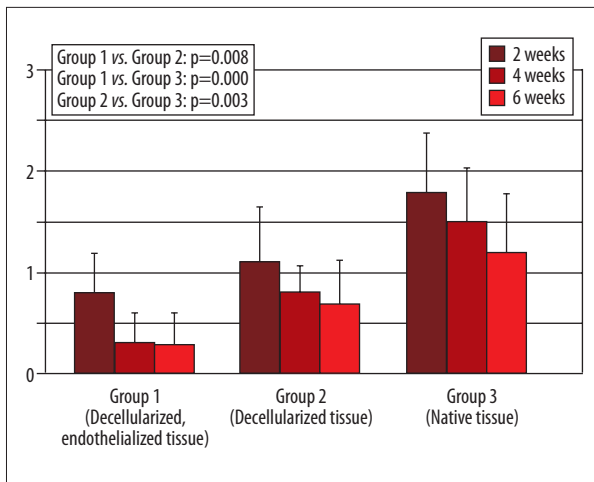


**Figure 1.** Monocyte infiltration in Hematoxylin-Eosin Staining. (Legend: 0=no infiltration, 1=low infiltration, 2=medium infiltration, 3=high infiltration, Error bar=confidence interval).

## Statistics

Semi-quantitative data was expressed as mean and standard deviation. Groups were compared with paired Wilcoxon tests and Friedmann tests. The level for statistical significance was set at p value <0.05. Data management and statistical analysis were done with IBM SPSS Statistics Version 20.0.

## Results

### Cultivation of EC and endothelialization of tissue specimens

The EC culture showed normal growth and after approximately two weeks a 25 cm<sup>2</sup> monolayer of EC was obtained. EC were used to endothelialize tissue specimens as described above. To control endothelialization, 10 Giemsa-stainings were performed, which all showed an EC monolayer on examined specimens.

### Gross examination

The strongest inflammatory reaction was seen in native aortic wall specimens after 2 weeks. Decellularized specimens and decellularized/endothelialized specimens showed a low inflammatory reaction without a difference between the groups. At 4 and 6 weeks after implantation, there was no macroscopic inflammatory reaction present in any group.

### Histological results

Histological evaluation revealed different results for the former intimal and adventitial side of the aortic tissue and the cutting

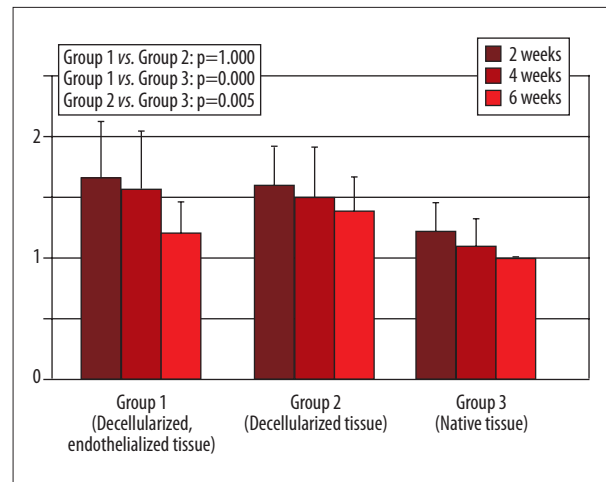


**Figure 2.** Fibroblast infiltration (0=no infiltration, 1=low infiltration, 2=medium infiltration, 3=high infiltration, Error bar=confidence interval).

edge of the tissue specimens. The following results of groups I, II, and III apply to the former intimal side of the implanted tissue. This side was chosen for prime analyses because of its major role in a tissue-engineered heart valve.

### Group 1 (decellularized/endothelialized specimens)

Cellular infiltration in this group was low at 2 and 4 weeks after implantation and decreased even more 6 weeks after implantation, with a significant difference in group 3 (p=0.000) and no difference in group 2 (p=0.145). Monocyte infiltration was also low, decreased more at 4 weeks after implantation, and stayed comparable at 6 weeks after implantation (Figure 1). Statistical analysis revealed a significantly lower infiltration with monocytes than in group 3 (p=0.000). Fibroblast infiltration was high and decreased at 4 weeks and 6 weeks after implantation, respectively (Figure 2). Analysis showed a significantly higher infiltration with fibroblasts than in group 3 (p=0.005) and no difference in group 2 (p=1.000). Surrounding the tissue specimens, many blood vessels were found (Figure 3), which was constant for the different explantation points and significantly higher than in group 2 (p=0.001) and group 3 (p=0.005).

### Group 2 (decellularized specimens)

Cellular infiltration in this group was low, with a significant difference in group 3 (p=0.000). It decreased at 4 and 6 weeks after implantation. Monocyte infiltration was also low and decreased at 4 and 6 weeks after implantation (Figure 1). A significant difference in Group 3 could be found (p=0.003). Fibroblast infiltration was high and decreased at 4 and 6 weeks after implantation (Figure 2). A significantly higher infiltration than in group 3 was found (p=0.005). There were few blood vessels surrounding the tissue specimens, which increased 4 weeks

after implantation before it decreased 6 weeks after implantation (Figure 3). The amount of blood vessels was comparable to group 3 ( $p=0.285$ ).

### Group 3 (native specimens)

Cellular infiltration in this group was high and decreased 4 to 6 weeks after implantation. Monocyte infiltration also was high and decreased 4 to 6 weeks after implantation (Figure 1). At 2 weeks, fibroblast infiltration was low and decreased thereafter (Figure 2). At 2 and 4 weeks after implantation, there were many blood vessels surrounding the tissue specimens, which decreased after 4 weeks (Figure 3).

### Histological results at the cutting edge and the former adventitial side of the tissue specimens

Cellular infiltration in Hematoxylin-eosin staining, CD 68 staining, and fibroblast staining higher was in all specimens at the cutting edge of the porcine aortic wall than at the former intimal aortic side. The former adventitial side showed a cellular infiltration in between the cutting edge and the former intimal side. This infiltration decreased the longer the tissue specimens were *in situ*. Decellularized specimens showed a lower cellular infiltration at the cutting edge and former adventitial side than native tissue specimens. The amount of blood vessels surrounding the tissue specimens was not different at the cutting edge and the former adventitial side or intimal side.

## Discussion

Recellularization of the scaffold is the key to creating a viable tissue-engineered heart valve. Various animal models are used to analyze migration of cells and their impact on the tissue. Assessment of cellular infiltration in rat subdermal models has been previously reported [9] but not yet with the implementation of tissue engineering and non-fixed biologic tissue. Figure 4A shows that the amount of cellular infiltration can be demonstrated very well. In our study, morphologically, the main part of cellular infiltration consisted of various types of leukocytes. Staining for monocytes, which are among the first cells involved in inflammatory responses, confirmed this. Of course, several types of monocytes are also important in constructive or regenerative processes [10]. From the detection of monocytes as used in this work, no conclusion can be made about their function. Nonetheless, monocytes are believed to be mainly destructive. Combined with the mostly leukocytic infiltration observed in Hematoxylin/eosin-staining in this study, a stronger infiltration with monocytes indicates more inflammatory response. Decellularized specimens (Group 1 and Group 2) compared to native specimens (Group 3) showed significantly

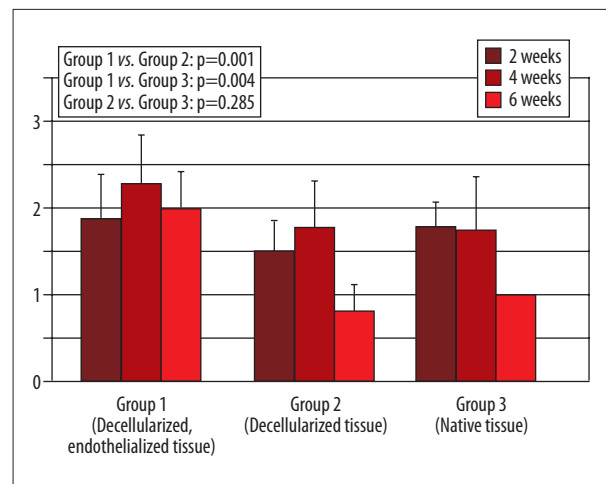


**Figure 3.** Density of blood vessels (Meaning per 1:400 lens coverage: 0=no vessels, 1=1–4 vessels, 2=4–8 vessels, 3=more than 8 vessels, Error bar=confidence interval).

lower infiltration of macrophages (Figure 1), which means lower antigenicity in the decellularized tissue specimens. The decrease of inflammatory reaction from 2 to 6 weeks points to a reduction of antigenic structures. Meyer et al. showed in an allograft model that decellularization also significantly reduced cellular and humoral immune response to allograft tissue [11]. Data obtained in this study relates to the published results of Erdbruegger et al. [4], who indicates that reduction of antigenic structures accompanies better structural integrity and functionality.

Furthermore, there was a higher infiltration at the cutting edge of the specimens. Various publications reported the antigenic potential of fragmented or damaged collagen [12,13]. This could, along with the disintegration of the extracellular matrix (ECM), cause the stronger infiltration with inflammatory cells. Data shows that reduction of the antigenic structures due to decellularization only works by the extraction of cellular components. ECM does not become altered nor does the collagen get cross-linked, so damaged collagen persists as antigenic structure. Therefore, Courtman, suggested that cross-linking procedures could be useful after decellularization [14].

Infiltration of fibroblasts was significantly higher in the decellularized specimens than in the native specimens. Endothelialization had no significant impact. Immigration of fibroblasts occurs for several reasons. The migration is induced by various factors produced by surrounding tissue cells. Fibroblasts migrate during inflammatory reactions and during tissue reconstruction after tissue trauma. In tissue-engineered heart valves, fibroblasts are thought to adapt to the environment of the heart valve. Thereby, fibroblasts can regenerate and remodel the decellularized tissue. In our experiment, the detection of fibroblasts was carried out by the

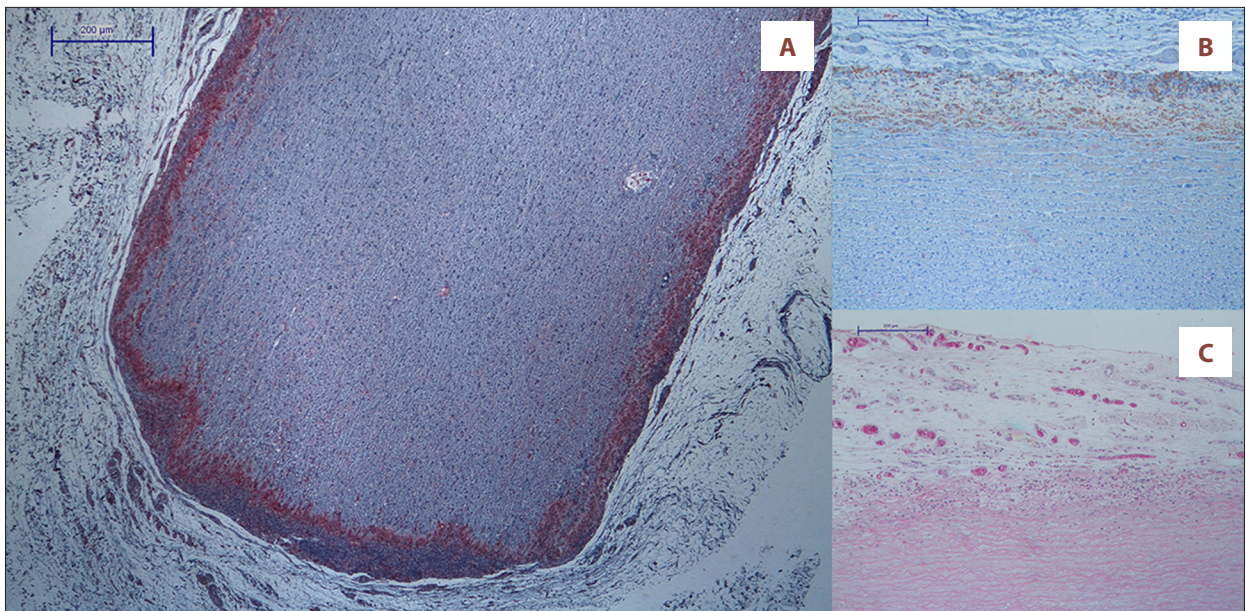


**Figure 4.** (A) Hematoxylin-eosin staining of decellularized aortic specimen (Group 2, right: former Intima, left: former Adventitia, bottom: cutting Edge) with low cellular infiltration. (B) CD-68 staining of decellularized aortic specimen (Group 2) with low infiltration of monocytes at the former intimal side of the vessel. (C) High density of blood vessels surrounding endothelialized tissue specimen (Group 1).

staining of prolyl-4-hydroxylase. This enzyme is directly related to the amount of produced collagen. Therefore, the detection of fibroblasts in this study cannot determine if fibroblasts migrated during inflammation or tissue regeneration. The different fibroblast infiltration in decellularized and the native tissue, in spite of a different inflammatory reaction in the various groups, points towards dissimilar causes of migration. The significantly higher amount of fibroblasts in decellularized tissue shows that there is no cytotoxic effect of the decellularization process but further conclusions would only be speculative.

The endothelial layer in blood vessels and heart valves regulates, among other things, cell migration. Also, an impact on calcification of biological heart valves was described [15]. *In vitro* endothelialization could therefore increase the recellularization of decellularized tissue and prevent calcification. In this study we showed unproblematic harvesting and cultivation of EC. Endothelialization of xenogenic tissue and implantation in the rat subdermal model was likewise unproblematic. Nonetheless, after explantation no confluent monolayer of EC could be observed. On the contrary, in a juvenile sheep model such a monolayer was observed [16] due to the subdermal position of the tissue specimens. Growth of EC is controlled by various cellular and extracellular substances produced by surrounding tissue [17]. Dependency between structure and function in growth and alignment of EC [18] results in augmented angiogenesis or formation of an EC monolayer. Therefore, growth of EC is different in blood stream and in a subdermal

position. The augmented blood vessel density surrounding the *in vitro* endothelialized tissue (Figure 4C) is direct consequence of this. Figure 3 shows also that this effect is persistent over the different implantation intervals. In contrast, the large number of blood vessels surrounding the native aortic wall specimens is caused by the inflammatory reaction. Therefore, blood vessel density declines at 6 weeks after implantation, and after the cellular debris is phagocytized the inflammatory reaction decreases. The higher number of blood vessels in Group 1 probably leads to a regression of cellular infiltration and monocyte infiltration (Figure 4B) due a quicker degradation of antigenic structures mediated by better microcirculation. To evaluate effects of an EC monolayer on decellularized tissue, other study setups, involving mechanical stress and positioning in the blood stream, must be considered.

## Conclusions

The subdermal model provides permanent contact of implanted tissue to host-tissue and sufficient blood supply, which eases cellular infiltration. The model allows observing the response to implanted tissue in a fast and authentic way. The subdermal position with the absence of blood stream and mechanical stress influences the cellular infiltration of implanted tissue. Therefore, endothelialization as used in this model does not lead to an endothelial monolayer, serving as a barrier between the implanted tissue and the test animal. Instead, it leads to increased vascularization surrounding the

tissue specimens. Due to these limitations, the rat subdermal model can only provide basic information about immunologic reactions and recellularization. Conclusions about biological compatibility can be made, but further questions regarding functionality cannot be answered and must be researched with other models.

## References:

1. Schoen FJ, Levy RJ: Founder's Award, 25<sup>th</sup> Annual Meeting of the Society for Biomaterials, perspectives. Providence, RI, April 28–May 2, 1999. Tissue heart valves: current challenges and future research perspectives. *J Biomed Mater Res*, 1999; 47(4): 439–65
2. Dohmen PM, Hauptmann S, Terytze A, Konertz WF: *In-vivo* repopularization of a tissue-engineered heart valve in a human subject. *J Heart Valve Dis*, 2007; 16(4): 447–49
3. Dohmen PM, Ozaki S, Yperman J et al: Lack of calcification of tissue engineered heart valves in juvenile sheep. *Semin Thorac Cardiovasc Surg*, 2001; 13(4 Suppl.1): 93–98
4. Erdbrügger W, Konertz W, Dohmen PM et al: Decellularized xenogenic heart valves reveal remodeling and growth potential *in vivo*. *Tissue Eng*, 2006; 12(8): 2059–68
5. Rashid ST, Salacinski HJ, Hamilton G, Seifalian AM: The use of animal models in developing the discipline of cardiovascular tissue engineering: a review. *Biomaterials*, 2004; 25(9): 1627–37
6. Dohmen PM, da Costa F, Lopes SV et al: Successful implantation of a decellularized equine pericardial patch into the systemic circulation. *Med Sci Monit Basic Res*, 2014; 20: 1–8
7. Mako WJ, Shah A, Vesely I: Mineralization of glutaraldehyde-fixed porcine aortic valve cusps in the subcutaneous rat model: analysis of variations in implant site and cuspal quadrants. *J Biomed Mater Res*, 1999; 45(3): 209–13
8. Dohmen PM, Meuris B, Flameng W, Konertz W: Influence of ischemic time and temperature on endothelial cell growth after transport. *Int J Artif Organs*, 2001; 24(5): 281–85
9. Abolhoda A, Yu S, Oyarzun JR et al: No-react detoxification process: a superior anticalcification method for bioprostheses. *Ann Thorac Surg*, 1996; 62(6): 1724–30
10. Asahara T, Murohara T, Sullivan A et al: Isolation of putative progenitor endothelial cells for angiogenesis. *Science*, 1997; 275(5302): 964–67
11. Meyer SR, Nagendran J, Desai LS et al: Decellularization reduces the immune response to aortic valve allografts in the rat. *J Thorac Cardiovasc Surg*, 2005; 130(2): 469–76
12. Grabenwöger M, Grimm M, Eybl E et al: New aspects of the degeneration of bioprosthetic heart valves after long-term implantation. *J Thorac Cardiovasc Surg*, 1992; 104(1): 14–21
13. Madri JA: Extracellular matrix modulation of vascular cell behaviour. *Transpl Immunol*, 1997; 5(3): 179–83
14. Courtman DW, Errett BF, Wilson GJ: The role of crosslinking in modification of the immune response elicited against xenogenic vascular acellular matrices. *J Biomed Mater Res*, 2001; 55(4): 576–86
15. Liao K, Gong G, Hoffman D et al: Spontaneous host endothelial growth on bioprosthetic valves and its relation to calcification. *Eur J Cardio-Thorac Surg Off J Eur Assoc Cardio-Thorac Surg*, 1993; 7(11): 591–96
16. Dohmen PM, Ozaki S, Nitsch R et al: A tissue engineered heart valve implanted in a juvenile sheep model. *Med Sci Monit Int Med J Exp Clin Res*, 2003; 9(4): BR97–104
17. Ferrara N: Role of vascular endothelial growth factor in regulation of physiological angiogenesis. *Am J Physiol Cell Physiol*, 2001; 280(6): C1358–66
18. Butcher JT, McQuinn TC, Sedmera D et al: Transitions in early embryonic atrioventricular valvular function correspond with changes in cushion biomechanics that are predictable by tissue composition. *Circ Res*, 2007; 100(10): 1503–11

## Acknowledgement

We would like to thank Mrs. Krüger for assistance in animal surgery the and preparing and staining the histological sections, and Mrs. Führer and Mrs. Müller for taking care of the study animals.